Wind effects on long-span bridges: Probabilistic wind data format for buffeting and VIV load assessments

K Hoffmann[1,*], **R G Srouji**[1] **and S O Hansen**[1,2]

[1]Svend Ole Hansen ApS, Sankt Jørgens Allé 5C, 1615 Copenhagen V, Denmark
[2]SOH Wind Engineering LLC, 141 Leroy Road, Williston, VT 05495, USA

*Corresponding author: kho@sohansen.dk

Abstract. The technology development within the structural design of long-span bridges in Norwegian fjords has created a need for reformulating the calculation format and the physical quantities used to describe the properties of wind and the associated wind-induced effects on bridge decks. Parts of a new probabilistic format describing the incoming, undisturbed wind is presented. It is expected that a fixed probabilistic format will facilitate a more physically consistent and precise description of the wind conditions, which in turn increase the accuracy and considerably reduce uncertainties in wind load assessments. Because the format is probabilistic, a quantification of the level of safety and uncertainty in predicted wind loads is readily accessible. A simple buffeting response calculation demonstrates the use of probabilistic wind data in the assessment of wind loads and responses. Furthermore, vortex-induced fatigue damage is discussed in relation to probabilistic wind turbulence data and response measurements from wind tunnel tests.

1. Introduction

The assessment of expected environmental loads is a key element in the design of engineering structures, influencing the complete chain of load carrying capacity analyses. Most often, the evaluation of governing loads utilizes codified mathematical models and site-specific environmental properties as input parameters. Several models and input parameters are required to cover all structural configurations and the associated risk categories and criteria, extending from the initial construction phase to the complete operational structure. The estimation of probabilities of events that are rare, but not necessarily extreme, is also important for serviceability evaluations.

The large dimensions and distinctive structural dynamics of many modern high-rise and long-span structures often challenge the traditional codified calculation frameworks. This may be manifested by excessive simplifications of the physical and mathematical load/response modelling or inadequate and insufficient descriptive parameters quantifying the environmental input. As a result, the load estimates may be unnecessarily conservative or even fail to capture specific relevant events. In any case, the level of safety in predicted environmental loads and associated structural responses may be very difficult to quantify utilizing traditional approaches.

Detailed information about expected environmental loads is naturally a requirement to obtain an optimal and safe design of any engineering structure. For bridges with span lengths larger than 300 m or natural frequencies below 0.5 Hz wind measurements at bridge site are actually mandatory [1]. The

focus of this paper is limited to the assessment of dimensioning buffeting loads and vortex-induced vibrations (VIV), and the associated physical parameters and predictive models.

Within the field of bridge aerodynamics, the fundamental mathematical models were developed more than 50 years ago, where the somewhat limited wind data sources primarily consisted of manually assisted recordings of very few parameters with a rather large spatial and temporal spacing. This is in contrast to present-day automated high-frequency data sampling from globally distributed networks of meteorological weather stations.

The considerable development in advanced wind sensors for measurement campaigns is also important. In the 1980s, cup anemometers were common, and today these are replaced by ultrasonic anemometers. In recent years, the wind characteristics in several Norwegian fjords have been investigated using scanning LIDARs [2]. This has enabled a wind field description with a high spatial and temporal resolution, which was previously impossible to acquire with cup anemometers. In order to fully exploit a probabilistic wind data format, a large amount of wind data measurements are needed on site, i.e. long time series at representative locations. Processing of large amount of data is no longer considered as a limitation as computer software and hardware are continuously being more powerful.

A generally accepted probabilistic wind data format will facilitate that measurements carried out in different Norwegian fjords and at other locations around the world may all contribute to a common database enabling easy comparisons and increased certainty in wind flow descriptions.

2. Wind load assessment

The engineering practice of predicting wind loads on structures is traditionally based on a calculation framework utilizing a combination of site-specific wind characteristics, structural properties, and mathematical models of their interaction. This framework may be visualized by the so-called wind loading chain, introduced by A. G. Davenport in the 1960s; see Figure 1. The concept of the chain illustrates that the different parts of the load assessment are interrelated, and that the reliability of an estimated wind load is at most as large as the least reliable link in the chain.

Figure 1 includes illustrations of fundamental probabilistic distributions representing the uncertainties and stochastic nature of models and parameters associated with each link. The focus of the present paper is probabilistic distributions modelling the wind climate, terrain effects, and the flow to pressure mechanisms, represented by the first three links.
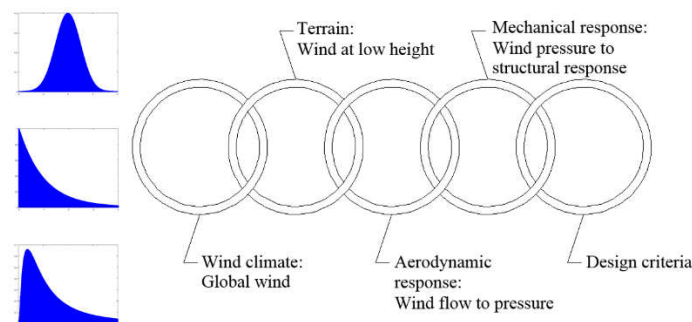

Figure 1. Principal sketch of the wind load design process, as illustrated by the wind loading chain, and different probabilistic distributions related to the uncertainties and stochastic nature of models and parameters associated with each link.

All parts of the wind loading chain consist of stochastic phenomena and simplified mathematical model relations associated with uncertainties. A deterministic approach is, however, often adopted for traditional structures due to its simplicity, since the key features of the wind load generation are often captured when the wind load model framework is calibrated against common load/response characteristics and experience from similar structures. In this framework, the conversion from

characteristic values to rare events is attained by partial factors calibrated to the generally accepted level of structural safety. On the other hand, a deterministic approach is often inadequate to assess the extreme wind loads on structures with non-traditional structural dynamics or extreme spatial dimensions. Instead, the wind load calculation format may be extended to cover the actual stochastic phenomena involved, which could not only increase the accuracy in predicted wind loads, but also capture wind effects, which are not covered by the traditional deterministic description. Additionally, the level of safety and uncertainty is implicitly part of the predicted wind loads. The increasing amount of wind data availability for many sites facilitates such a probabilistic description of the governing wind phenomena.

3. Stochastic nature of wind

The description of wind turbulence is of crucial importance for the prediction of fluctuating wind loads on structures. The typical procedure is to model the wind turbulence description by the following site-specific wind data input:

- Turbulence intensities;
- Integral length scales;
- Power-spectral density functions;
- Normalized co-spectra.

The wind data traditionally consist of deterministic parameter values and model functions evaluated at the design mean wind velocity. This is also the underlying wind turbulence description utilized in many wind codes [1], [3] and forms the basis of principles for safety and serviceability of structures [4]. Suggested parameter and model values exist in both wind norms, however, these are not intended to be used for long-span bridge dimensioning without further justification.

Wind data from Horns Rev is utilized in the following section to illustrate the stochastic nature of wind turbulence. The Horns Rev site is located at a reef approx. 14 km off Jutland, west of Denmark, in a very harsh offshore environment. The wind measurements are 12 Hz samples and cover a period of approx. 5 years (2001-2005) and originate from a 3D sonic anemometer positioned 50 m above sea level. Since the site is open waters, a terrain roughness length of approx. 0.003 m may be assumed for high wind velocities. The wind measurements include some time gaps where recordings were not performed. The complete data set consists of 112586 time-series of 10-min duration.

3.1. Turbulence intensity

The relative extent of the along-wind velocity fluctuations at a certain mean wind velocity is represented by the turbulence intensity

$$I_u = \frac{\sigma_u}{U},$$ (1)

where σ_u is the standard deviation of the along-wind turbulence component u and U is the 10-min mean wind velocity. Codified models prescribe a single value of turbulence intensity based on the terrain roughness length and the elevation, implicitly referring to turbulence intensity at high wind velocities [1], [3].

Figure 2 presents wind turbulence intensities measured at Horns Rev. The plot illustrates a few key features related to the stochastic nature of the turbulence intensity. Generally, the scatter is large, especially at low and moderate wind velocities, where the variability of thermal stratification strongly influences the mechanically generated turbulence. Conditions with nominally zero turbulence intensity do only occur at wind velocities, say, below 10-15 m/s, while larger wind velocities seem to ensure a certain amount of wind turbulence. This observation is relevant for the assessment of possible VIV, where wind turbulence components reduce the critical fatigue loads. Similarly, provisions such as Eurocode 1 prescribe a reduction in VIV loads at high wind velocities. At high wind velocities above 20 m/s, where buffeting loads are of importance, the turbulence intensity is in the range 5 - 20 %.
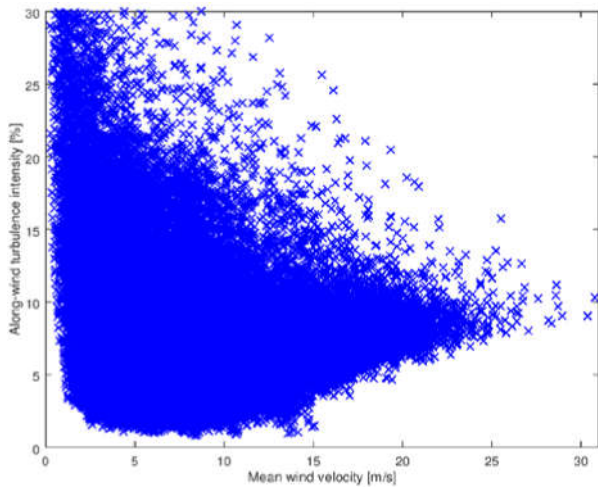
Figure 2. Along-wind turbulence intensity as a function of the 10-min mean wind velocity measured at Horns Rev.
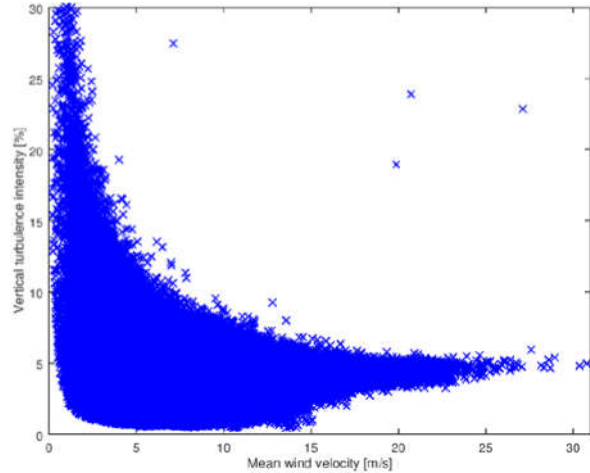
Figure 3. Vertical turbulence intensity as a function of the 10-min mean wind velocity measured at Horns Rev.

The codified value of the along-wind turbulence intensity at the site is approx. 10.3 % [3]. This is an underestimation of the turbulence intensity for some of the extreme events seen in Figure 2. Utilizing the codified prescription without safety factors may in such cases result in underestimated buffeting loads.

The vertical turbulence intensity σ_w/U is presented in Figure 3. Generally, the vertical turbulence intensity seems to produce less scatter than the along-wind turbulence intensity, except for very few outliers. Conditions with nominally zero turbulence intensity seem to occur only at wind velocities, say, below 15 m/s, while larger wind velocities seem to ensure a certain amount of wind turbulence. The vertical turbulence intensity seems to approach approx. 5 % at high wind velocities. This is in agreement with $I_w \approx 0.5I_u$, which is a typical approximation to apply for design purposes [5].

In the field of bridge aerodynamics, low-intensity turbulence conditions at moderate wind velocities is generally governing VIV and possible fatigue damage, while high-intensity turbulence conditions at high wind velocities are dimensioning for buffeting responses. The following subsections will consider these two scenarios and, by examples, illustrate simple probabilistic model relations of the along-wind turbulence intensity.

3.1.1. Low-intensity turbulence at moderate wind velocities. Figure 4 illustrates the distribution of measured along-wind turbulence intensities for mean wind velocities in the interval 5 - 10 m/s. As a first approximation, a gamma distribution is fitted to model the low-turbulence conditions. The gamma probability density function is defined by

$$f_{\text{gam}}(x) := \frac{\beta^{\alpha} x^{\alpha-1} \exp(-\beta x)}{\Gamma(\alpha)}, \tag{2}$$

where α is the shape parameter, β is the rate parameter, and Γ is the gamma function. The fitted distribution corresponds to a shape parameter of 8.0 and rate parameter of 0.8 %.

For a structure prone to VIV, the cumulative fatigue damage may be calculated utilizing the probability distribution of low turbulence intensity events near the critical wind velocity to assess the risk of fatigue failures.

3.1.2. High-intensity turbulence at high wind velocities. Figure 5 shows the distribution of measured along-wind turbulence intensities for mean wind velocities above 15 m/s.

As a first approximation, an exponential distribution is fitted to model high-turbulence conditions. The exponential distribution is a special type of gamma distribution, and the probability density function is

$$f_{\mathrm{exp}}(x) := \beta \exp(-\beta x), \tag{3}$$

where β is the rate parameter. Note that the mean value of the distribution is $1/\beta$ and this will in the following be used to describe the distribution. In the present model framework a translation is also introduced, which corresponds to replacing x by $x - x_0$ for a translation of x_0.

The fitted distribution of high-turbulence conditions above 8 % corresponds to a mean value of 1.5 % and translation of 6.5 %. This is an example of a probabilistic distribution modelling conditions corresponding to critical buffeting loads.
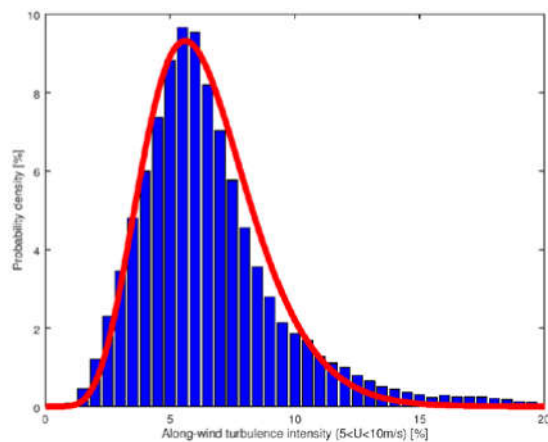

Figure 4. Distribution of measured along-wind turbulence intensities for mean wind velocities in the interval 5 - 10 m/s. Each bar represents the probability for a turbulence intensity interval of 0.5 %. A gamma distribution with a shape parameter of 8.0 and a rate parameter of 0.8 % is fitted to model the low-turbulent conditions below 5 %.
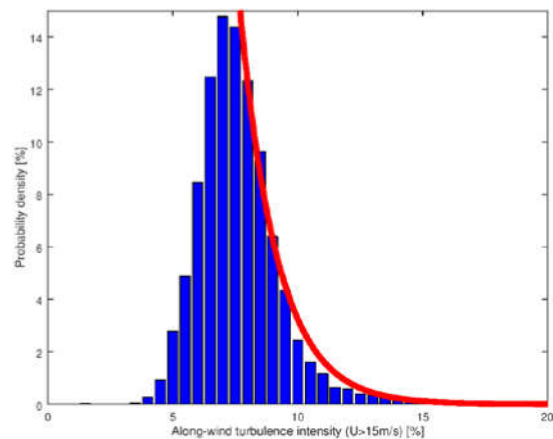
Figure 5. Distribution of measured along-wind turbulence intensities for mean wind velocities above 15 m/s. Each bar represents the probability for a turbulence intensity interval of 0.5 %. An exponential distribution with a mean value parameter of 1.5 % and a translation of 6.5 % is fitted to model the high-turbulent conditions.

3.2. Integral length scale

The integral length scale is a measure of the correlation of along-wind turbulence components, and is used in the traditional modelling framework to prescribe the frequency with the largest turbulent energy at a given mean wind velocity. Integral length scales may be determined by applying Taylor's hypothesis to the time scale found using the auto-correlation function of the along-wind component at a single point [5]. If the process involves time integration of finite measurement periods not much larger than the corresponding time scale, a filtering process, such as the Blackman-Tukey method, should be considered to reduce the error variance, i.e. to avoid an overestimation of the auto-correlation at large time lags [6].

Figure 6 shows the distribution of the integral length scale for along-wind turbulence L_u^x determined by the procedure explained above without the use of a filtering process. As a first approximation, an exponential distribution with a mean value of 125 m has been fitted to model the upper tail of the distribution. By comparison, at the elevation and terrain roughness length of the measurement site, the codified value of the along-wind integral length scale is approx. 177 m [3].
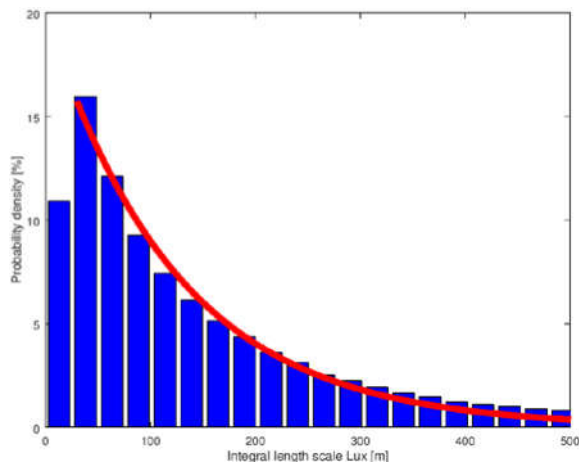
Figure 6. Distribution of measured longitudinal integral length scales for all mean wind velocities. Each bar represents the probability for a length scale interval of 25 m. The fitted exponential distribution with a mean value of 125 m seems to provide a good model of the distribution of integral length scales above approx. 30 m.
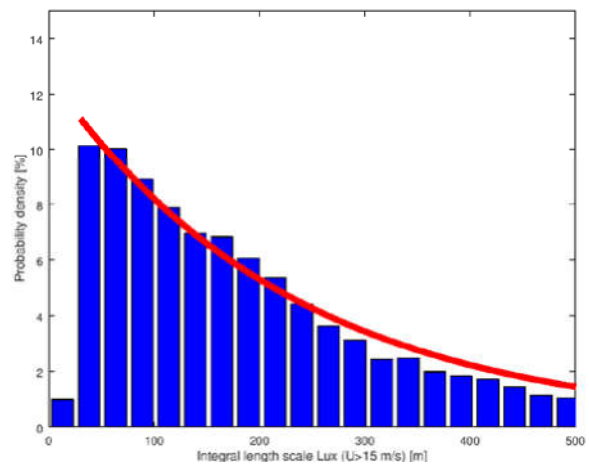
Figure 7. Distribution of measured longitudinal integral length scales for 10-min mean wind velocities above 15 m/s. Each bar represents the probability for a length scale interval of 25 m. The fitted exponential distribution with a mean value of 230 m and a translation of 35 m seems to provide a good model of the distribution of integral length scales above approx. 35 m.

A simple model of the integral length scale at high wind velocities may be estimated by a similar fitting procedure. Figure 7 illustrates such a distribution restricted to 10-min mean wind velocities above 15 m/s. The average integral length scale increase at high wind velocity conditions. The presented exponential fit with a mean value of 230 m and a translation of 35 m approximates the distribution for length scales above approx. 35 m.

3.3. Power-spectral density function
The frequency wise distribution of turbulent energy is modelled by the power-spectral density function. In the Eurocode 1 [3] and Håndbok N400 [1] prescriptions, the normalized single-point power-spectral density is modelled by the expression

$$R_{\mathrm{N,EC1}}(n) := \frac{nS_{u,\mathrm{EC1}}(n)}{\sigma_u^2} = \frac{6.8f_L}{(1+10.2f_L)^{5/3}}, \tag{4}$$

where n is the frequency and $f_L := nL_u^x/U$ is the normalized frequency. The presented spectrum is of the Kaimal spectral density form and focuses on a consistent modelling of the high-frequency behavior. The Kaimal spectrum satisfies Kolmogorov's law for the energy distribution in the turbulent fluid. The spectrum shape is fixed, and the integral length scale and the mean wind velocity prescribe the frequency with the largest normalized turbulent energy.

The point-wise power-spectral density at a given location may also be estimated by analyzing wind velocity measurements. This requires a high sampling rate to capture the high-frequency part. Measurements from the first 24 hours of 2002 have been used to produce an example of the spectral density of the turbulence components. This corresponds to approx. 1 million data points given the 12 Hz sampling rate. The power-spectral density of each 10-min block is calculated, and the mean value for each frequency component of these 144 spectra is determined. The power-spectral density above $n = 3$ Hz has been discarded to remove most effects of spectral folding. The normalized frequency is determined using the 10-min mean wind velocity in each 10-min block, varying from 5 to 20 m/s during this specific day. The integral length scale for the along-wind and vertical turbulence model is set to 125 m and 12.5 m, respectively. The normalization of R_{N} for the vertical turbulence is performed using σ_w^2. These two spectra and the Eurocode 1 spectrum are plotted in Figure 8.

The measurements show a good resemblance with the Eurocode 1 prescriptions. The spectrum of the vertical turbulence components seem to match the codified prescriptions by utilizing an integral length scale for the normalized frequency which is 1/10th of the along-wind integral length scale. Note that the actual integral length scale of the vertical turbulence component is likely different than this value. The 1/10 factor is here chosen to produce a model spectrum of the vertical turbulence, expressed by the codified along-wind spectrum.
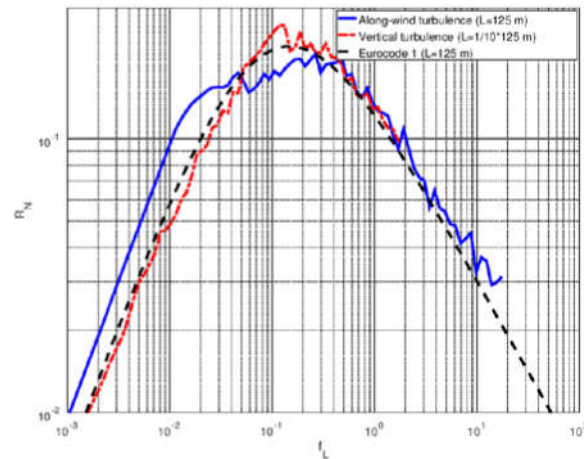

Figure 8. Spectra of measured along-wind and vertical turbulence. The integral length scale used for the normalized frequency is 125 m and 12.5 m, respectively. The black dashed curve is the Eurocode 1 spectrum for the along-wind turbulence with an integral length scale of 125 m.

The integral length scale is not constant during a day. It is therefore expected that a 1-day average spectrum based on a constant integral length scale will have energy redistributed from the peak value to smaller and larger frequencies, i.e. it will be more "flat". Such an effect is slightly visible for the along-wind turbulence spectrum in Figure 8.

The presented codified spectrum gives a frequency-wise representation of the fluctuating energy covering the dynamic effects of relevance for most structures, including modern bridges. In the case of unusual low-frequency dynamics, such as those associated with flexible offshore structures, a spectral representation tuned to match the low-frequency regime is required. For such structures, it is therefore recommended to rely on a different spectral description [7]. The buffeting load calculation presented in Section 5 will utilize a simple probabilistic distribution of the point-wise along-wind power-spectral density based on the codified spectrum.

3.4. Normalized co-spectra

The normalized co-spectrum models the statistical dependence between the turbulence at two points with a certain spatial separation. This statistical dependence is naturally closely related to the spatial dimension of vortices in the wind field. For the along-wind turbulence component, the normalized co-spectrum for two points of lateral separation r_y at a given frequency n_i may be modelled by the Davenport model [5]

$$\psi_u = \exp(-C_{uy} r_y n / U).$$

(5)

The non-dimensional decay constant C_{uy} is 10 according to the general prescriptions [1]. The stochastic nature of the normalized co-spectrum or the associated decay constant will not be further addressed in this treatment, but a probabilistic description is introduced as part of the example calculation presented in Section 5.

4. Probabilistic wind data provisions

The stochastic nature of wind turbulence should preferably be accounted for in a physically consistent manner, yet, several rather complicated physical phenomena are responsible for the wind turbulence generation under different climatic conditions. The lack of wind stationarity and the influence of the fetch are additional sources of uncertainty. As a result, the stochastic processes are difficult to model without applying certain simplifications.

The probabilistic models presented in the previous section do not necessarily reflect the physics behind turbulence generation. They are merely introduced as first approximation examples used to describe the governing wind data by standard distributions fitted to a single set of measurement data. These example distributions are also utilized in the example calculation performed in Section 5.

In its simplest form, a physically consistent stochastic wind turbulence model should account for the fact that turbulence at low wind velocities is primarily generated by thermal convection, while turbulence at higher velocities is primarily mechanically generated due to friction forces between the air and any irregular terrain and obstacles. Prescribed stochastic model representations of wind turbulence should therefore represent the distinct physics behind turbulence generation at different climatic conditions, as expressed by the stochastic processes. Such modelling is outside the main field of expertise of the authors, and a consistent treatment of this topic requires further involvement of meteorologist, measurement equipment manufacturers and end-users, and data statisticians.

As mentioned previously, in the field of bridge aerodynamics, wind turbulence at low wind velocities is generally governing VIV, while high-wind turbulence conditions are dimensioning for buffeting responses. A probabilistic assessment of the associated governing structural loads requires probabilistic distributions of the following data:

- Turbulence intensities I_u, I_w as a function of U;
- Integral length scales L_u^x, L_w^y, as a function of U;
- Point-wise power-spectral densities S_u, S_w as a function of U;
- Decay constants C_{uy}, C_{uz}, C_{wx}, C_{wy} as a function of U;
- Mean wind velocity and velocity pressure U, q - Direction-dependent typical and extreme values;
- Air density ρ as a function of U;
- Mean wind inclination from horizontal as a function of U.

This list should be considered an initial provision. It may be advantageous to model some parameters in other formats. For instance, if the non-dimensional decay constants C are used in an exponential format, where they are multiplied by U^{-1}, probabilistic descriptions of C/U are just as useful. A better understanding of the governing wind phenomena, combined with analyses of measurement data, will indicate the type of quantities, which are advantageous to use in the probabilistic modelling. A well-defined probabilistic wind data format will also establish a common basis, promoting a direct comparison of wind data from different measurement sites.

5. Example - Probabilistic wind load assessment

To give an example of a probabilistic wind load assessment, the following section will consider the extreme resonant turbulent response of a simple horizontal line-like structure, positioned in a wind climate similar to the probabilistic descriptions presented in Section 3.

5.1. Buffeting load and response model

The power-spectral density of the resonant turbulent drag load on a line-like structure is given by the relation [5]

$$S_{\mathrm{drag}}(n) = \left(\frac{1}{2}\rho U h l\right)^2 (2C_{\mathrm{D}})^2 \left|J_u(n)\right|^2 S_u(n), \tag{6}$$

where h and l are the height and length of the structure, C_D is the drag coefficient, and S_u is the power-spectral density of the along-wind turbulence. The joint acceptance function is given by

$$|J_u(n)|^2 = \frac{1}{l^2} \int_0^l \int_0^l \xi(y_1)\xi(y_2)\psi_u(r_y, n)\, dy_1 dy_2,$$ (7)

where ξ is a mode shape in the direction in the wind. The mode shape is normalized to have a maximum value of 1. The cross-sectional aerodynamic admittance function for drag has been assumed to be 1. Thus, the lack of correlation of pressures on the front and suction on the back has been discarded for simplicity.

By utilizing the white noise approximation, the power-spectral density of the resonant turbulent drag load may be evaluated at a natural frequency n_i. This gives the variance of the corresponding maximum resonant structural acceleration, as expressed by [5]

$$\sigma_{\text{acc}}^2 = \frac{1}{m_i^2} \frac{\pi^2}{2\delta_i} n_i S_{\text{drag}}(n_i).$$ (8)

In the expression above, δ_i is the mode-specific sum of the aerodynamic and structural damping given by a logarithmic decrement (LD) and m_i is the generalized mass defined by

$$m_i = \int_0^l \mu(y)\, \xi_i^2(y)\, dy,$$ (9)

where μ is the structural mass per unit length.

The standard deviation of the structural acceleration σ_{acc} is the quantity to be estimated in the example calculation. In practical applications, the structural acceleration is usually determined to evaluate corresponding inertial loads, which ultimately are added to the mean and background turbulent loads to model an extreme load scenario.

5.2. Probabilistic wind data

The probabilistic distributions utilized for the wind data in the calculation example are listed in Table 1, including the example distributions for the high-wind turbulence intensity and integral length scales presented in Section 3.

Table 1. Probabilistic distributions for wind data used in the example calculation.

Parameter	I_u [%]	L_u^x [m]	$S_u(n_i)$ [m^2/s]	C_{uy} [-]	q [N/m^2]
Distribution type	Exp.	Exp.	Normal	Normal	Gumbel
Mean value	8.0 %[a]	265[a]	$S_{u,\text{EC1}}(n_i)$	10	-
Coeff. of variation	-	-	0.1	0.1	-
Location	-	-	-	-	465
Scale	-	-	-	-	93
Translation	6.5 %	35	-	-	-

[a] After translation.

The mean value of the single-point spectrum S_u at a given frequency is modelled by codified prescriptions [1], [3]. The spectral content at n_i is assumed to be normally distributed, with a coefficient of variation of 0.1. Note that the probabilistic nature of the spectrum is also governed by the probabilistic models of the turbulence intensity and integral length scale. The non-dimensional decay constant C_{uy} for the co-spectrum is assumed to be normally distributed with mean value 10 and coefficient of variation of 0.1. The mean value is in accordance with the prescriptions of Håndbok N400 [1]. The annual extreme 10-min mean wind velocity is implicitly modelled by a Gumbel distribution for the annual extreme mean velocity pressure. The listed Gumbel parameters follow the prescriptions of the Danish national annex of Eurocode 1 and correspond to a 50-year basic wind velocity of 24 m/s, an elevation of 50 m, and a

terrain roughness length of 0.003 m. The air density is set to 1.25 kg/m^3 in all the example calculations. It is for simplicity assumed that the direction of the wind is always perpendicular to the structure.

5.3. Structural data

The present probabilistic framework focuses on climatic parameters. All structural parameters are therefore, for simplicity, defined by deterministic values to illustrate the effect of a probabilistic wind data format alone. For the present example, the values listed in Table 2 are applied.

Table 2. Deterministic structural data used in the example calculation.

h	l	C_D	μ	m_i	n_i	ξ_i	δ_i
1 m	100 m	1.0	1,000 kg/m	50,000 kg	1.0 Hz	$\sin(\pi y/l)$	3 % LD

For most practical applications, the structural parameters have a varying level of uncertainty. For example, often the geometry and mass of the structure are both known quite accurate, while the structural dynamics is governed by a relatively large uncertainty.

5.4. Probabilistic extreme resonant turbulent response

The buffeting load and response model has been evaluated numerically using the probabilistic wind data input to produce 10^8 realizations of the yearly extreme horizontal structural acceleration caused by resonant buffeting loads. The associated distribution is illustrated in Figure 9.
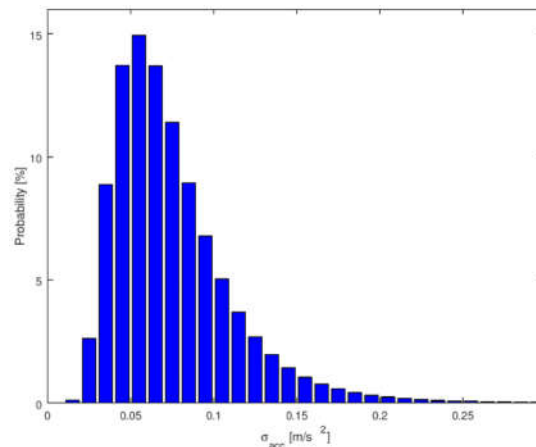

Figure 9. Distribution of yearly extreme standard deviation acceleration due to resonant buffeting loads. Each bar represents the probability for an interval of 0.01 m/s. The plot window covers approx. 99.9 % of the realizations.

The extreme horizontal accelerations associated with different return periods are listed in Table 3, where the yearly probability of a T-year response is defined by 1-exp(-1/T) [5].

Table 3. Estimated extreme horizontal accelerations for different mean return intervals (MRI).

MRI, T [years]	1	50	100	500	1000	5000	10000
$\sigma_{\text{acc},T}$ [m/s^2]	0.058	0.175	0.200	0.263	0.292	0.368	0.403

The ratio between the 50-year extreme value and larger mean return periods is illustrated in Figure 10. Note that the ratio between the resonant turbulent response and the mean response increases with the return period. While the mean response scales with the square of the mean wind velocity, an increased mean wind velocity also increases load correlation and relative fluctuating energy at the resonant frequency for the present example structure. In the calculation framework, this is manifested by an additional increase in the joint acceptance function and the point-wise power-spectral density of the along-wind turbulence.

The traditional deterministic assessment of a 50-year extreme response is based on codified models of the turbulence intensity and integral length scale. In the present case, this corresponds to $I_u \approx 10.3$ % and $L_u^{\,x} \approx 177$ m [3]. Combined with the deterministic Eurocode 1 spectrum and a decay constant $C_{uy} = 10$, this produces a 50-year resonant response of 0.181 m/s^2. This is very similar to the 50-year response of 0.175 m/s^2 estimated in the probabilistic analysis; see Table 3.
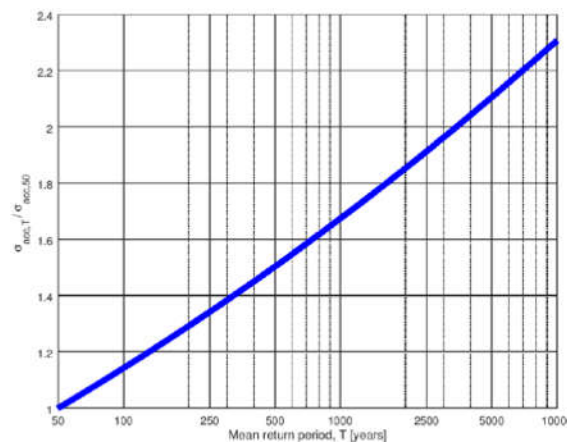

Figure 10. Ratio between 50-year extreme value and larger mean return periods.

Given the estimated extreme response probability distribution, it is straightforward to quantify the level of safety in the predicted responses, due to the correspondence between the return period and the probability of a yearly extreme event. However, it is important to remember that the relative uncertainty in the estimated response probability distribution increases for larger mean return periods. This means that a higher number of realizations is needed to accurately model the risk of extreme events for larger mean return periods.

6. Vertical load correlation for bridge decks

Vertical turbulence components are often the main source of dynamic vertical loads on bridge decks. To describe the interaction between vertical load components along the bridge, the lack of correlation between the generated surface pressures should be taken into account. The spectral response contribution from all pairs of surface points on such a plate-like horizontal structure may be expressed mathematically by an aerodynamic admittance function. In principle, this is nothing but a quadruple integral of all load pairs with a certain spatial separation along the two main axes of the bridge deck, quantifying the average lack of load correlation.

For high frequencies, the simple exponential format of the normalized co-spectrum given by Equation (5) may be adopted. It can then be shown theoretically that in the upper-frequency limit, the plate-like aerodynamic admittance function χ_{xy}^2 may be expressed using two line-like aerodynamic admittance functions χ_x^2, χ_y^2 according to the expression [5]

$$\left|\chi_{xy}(\phi_{xy})\right|^2 = \frac{\pi}{2}\left|\chi_x(\phi_x)\right|^2\left|\chi_y(\phi_y)\right|^2,$$

(10)

where $\phi_i = C_i n l_i / U$, utilizing the decay constant C_i, the frequency n, the structural dimension l_i, and the mean wind velocity U. This relationship has also been validated in wind tunnel experiments [8].

Since the line-like aerodynamic admittance function is inversely proportional to the frequency in the upper-frequency limit [5], [9], the expression may be reformulated as

$$\lim_{n\to\infty}\left|\chi_{xy}(\phi_{xy})\right|^2 = \left|\chi_x\left(\frac{2}{\pi}\phi_x\right)\right|^2 \left|\chi_y(\phi_y)\right|^2. \tag{11}$$

The calculation of the two-dimensional aerodynamic admittance function may therefore be significantly simplified in the upper-frequency range by using suitable products of a cross-sectional and a line-like aerodynamic admittance function. The fact that the load pair separations on plate-like structures cover a surface, and not just a line, is therefore included theoretically by a scaling of the argument in one of the aerodynamic admittance functions. The line-like aerodynamic admittance function describes the lack of correlation along the bridge deck, and this is governed by the correlation characteristics of the approaching undisturbed vertical wind velocity component. Thus, the planned full-scale measurements of the wind characteristics in the Norwegian fjords may readily be used in the format given by equation (11).

The simplicity of utilizing two aerodynamic admittance functions in buffeting load calculations for plate-like surfaces in the high-frequency range is a motivation for including such formats in codified prescriptions. It is expected that such a format is to be included in future revisions of Eurocode 1, concerning the buffeting loads on typical structures.

In relation to the aerodynamic modal forces on structures, a similar approach may be applied. In this case, one of the aerodynamic admittance functions quantifies the load correlation in terms of weighted modal loads and is, in principle, expressed by a joint acceptance function.

The simple exponential model in equation (5) is designed to model correlation at typical structural natural frequencies and spatial dimensions. For long-span bridges, the simple exponential modelling of the span-wise correlation of wind turbulence and the associated surface pressure fluctuations is therefore inconsistent given the relatively low natural frequencies and very large dimensions for such structures [10]. For instance, the modelled correlation approaches unity at very small frequencies, even at separations much larger than the average size of wind gusts.

A modified exponential format has been proposed, addressing some of the physical inconsistencies of the simple exponential model [11]. This format seems to provide a better representation, especially at large separations. Modern remote wind measurement systems, such as LIDARS, allow for site-specific large-separation correlation statistics. Further experience from such measurement campaigns will reveal the need for reassessing the modelling of the normalized co-spectrum for long-span bridges. In any case, the format given by equation (11) is valid for any type of large-separation correlation model.

7. Vortex-induced vibrations - Fatigue damage

VIV amplitudes larger than vibrations due to typical buffeting loads are often not accepted in the design criteria for modern long-span bridges. The bridge deck geometry is therefore often thoroughly tested, for instance in wind tunnel section model experiments, to ensure a sufficiently small-amplitude VIV response.

The principal physical phenomenon behind VIV is a motion-induced load in the form of a negative aerodynamic damping [5]. Large-amplitude VIV occur when the corresponding aerodynamic loads exceed the structural damping mechanisms. The aerodynamic load is reduced in the presence of along-wind turbulence components. Conditions with nominally zero wind turbulence cannot generally be discarded at typical mean wind velocities below approx. 15 m/s, similar to the turbulence data presented in Figure 2. The peak VIV amplitude, independent on its magnitude, is therefore generally to be expected on a sub-yearly basis, and experimental procedures should therefore be performed in low-turbulent conditions to outline the expected peak response. The estimated peak VIV amplitude is used in the assessment of serviceability and user comfort.

Extensive studies have shown that aerodynamic remedies in the form of guide vanes and a centrally located vortex spoiler may be an effective mean for suppressing VIV of bridge decks. For example, wind tunnel experiments previously carried out on a section model of the Hardanger Suspension Bridge have shown that simple aerodynamic remedies reduce the peak vertical vortex-induced response from approx. 15 % to approx. 3 % of the bridge deck height. Similar aerodynamic remedies have been retrofitted on a number of Norwegian and Danish bridges with spans varying from approx. 300 m to 1,600 m, significantly reducing the peak VIV response [12].

The probabilistic aspect of VIV modelling is primarily related to possible fatigue damage by modelling the occurrence of dynamic responses. For long-span bridges, which have relatively low natural frequencies, the bridge interaction with the vortex-shedding frequency may occur a large number of times throughout the bridge's lifetime due to the rather low critical wind velocity.

The VIV load reduction caused by non-zero along-wind turbulence is included in the Eurocode 1, Approach 2 format by a corresponding reduction of the aerodynamic damping parameter K_a [13]. An example of this is presented in Figure 11, where the codified normalized extreme VIV response is plotted as a function of the turbulence intensity for a representative streamlined bridge cross section with and without aerodynamic remedies.

A probabilistic model of low-intensity turbulence near the critical wind velocity, as the one presented in Figure 4, combined with a model of the VIV response as a function of the turbulence intensity, as the one presented in Figure 11, facilitates accurate predictions of load cycles and the corresponding fatigue damage for various structural elements on a bridge. Similarly, the fatigue damage reduction due to aerodynamic remedies is possible to quantify. A more advanced VIV response model could take into account the finite time of the amplitude build-up and decay, which for a long-span bridge may correspond to a time frame much larger than 10 min.
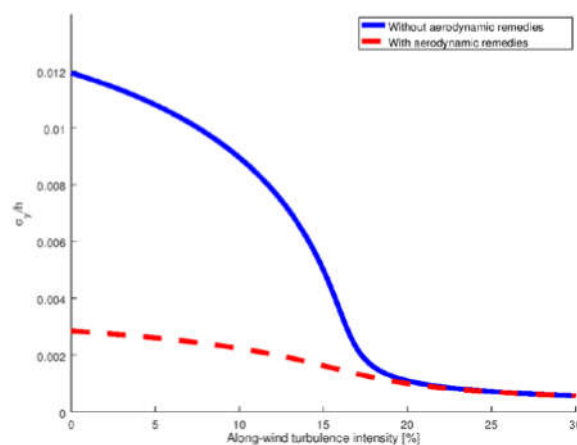

Figure 11. Principal interpretation of wind tunnel tests for a bridge section with and without aerodynamic remedies, illustrating the extreme normalized standard deviation as a function of the along-wind turbulence intensity.

8. Secondary aerodynamic loads

In addition to the mean and buffeting wind loads on a long-span bridge, there exist numerous aerodynamic loads, which are also assessed in the design phase. These loads are here denoted *secondary*, since they are assessed following the VIV, buffeting, and flutter aerodynamics due to their less fundamental influence of the bridge design. Secondary aerodynamic loads include cable loads and loads caused by special combined climatic effects, such as the accretion of ice or snow on bridge deck railings, changing the deck aerodynamics. Joint probability distributions of the wind velocity, direction, temperature, and rain/snow intensity may be utilized to assess such secondary effects. In addition, such distributions would allow for an assessment of the necessity of enforced traffic restrictions and bridge

closures due to strong winds. This may be used to evaluate the need of wind shields and their required efficiency.

9. Summary and conclusion

This paper presents initial suggestions for an extended probabilistic wind data format, which may be used to assess VIV and buffeting loads on long-span bridges.

The stochastic nature of wind turbulence is illustrated in a series of plots utilizing wind data from Horns Rev. Initial provision for a probabilistic wind data format applicable to long-span bridges is proposed. A wind load assessment on a simple line-like structure utilizing probabilistic wind data is presented in order to illustrate the main methodology, and how the probabilistic load assessment format establishes a one-to-one correspondence between extreme responses and return periods for a given site and structure. A future development of the extended probabilistic data format and associated wind load calculation frameworks will greatly benefit from continuous dialogue and collaboration between public road authorities, meteorological institutes, and wind load engineers.

Modern long-span bridge concepts will not be realized unless cost-effective design is an important part of the construction process. Wind loading is perhaps the most important environmental load governing the design of long span bridges. Therefore, all efforts invested in establishing safer and more accurate wind load models will be beneficial.

References

[1] Håndbok N400 – Bruprosjektering 2015 Norwegian Public Roads Administration
[2] Cheynet E, Jakobsen J B, Snæbjörnsson J, Reuder J, Kumer V and Svardal B 2017 Assessing the potential of a commercial pulsed lidar for wind characterisation at a bridge site *J. of Wind Engineering and Industrial Aerodynamics* **161** pp 17-26
[3] DS/EN 1991-1-4:2007, Eurocode 1: Actions on structures – Part 1-4: General actions – Wind actions 2007 Dansk Standard, Denmark
[4] DS/EN 1990:2007, Eurocode 0: Basis of structural design, 2007, Dansk Standard, Denmark
[5] Dyrbye C and Hansen S O 1997 *Wind loads on structures*, John Wiley & Sons Ltd.
[6] Zaknich A 2005 *Principles of Adaptive Filters and Self-learning Systems. Advanced Textbooks in Control and Signal Processing*, Springer
[7] Højstrup J, Larsen S E and Madsen P H 1990 Power spectra of horizontal wind components in the neutral atmospheric surface boundary layer *AMS 9th Symp. on Turbulence and Diffusion* Roskilde, Denmark pp 305–8
[8] Hoffmann K, Srouji R G and Hansen S O 2016 Buffeting loads on high-rise and long-span structures *8th Int. Colloquium on Bluff Body Aerodynamics and Applications*, Boston, USA
[9] Davenport A G 1977 The prediction of the response of structures to gusty wind *Safety of structures under dynamic loading* ed 1 pp 257–84
[10] Srouji R G, Hoffmann K and Hansen S O 2017 Experimental verification of a generic buffeting load model for high-rise and long-span structures *The 7th European and African Conf. on Wind Engineering* Liege, Belgium
[11] Krenk S 1996 Wind field coherence and dynamic wind forces *Solid mechanics and its applications* **47** pp 269–78

[12] Hansen S O, Srouji R G, Isaksen B and Berntsen K 2015 Vortex-induced vibrations of streamlined single box girder bridge decks *14th International Conference on Wind Engineering* Porto Alegre, Brazil

[13] Hansen S O 2017 Vortex-induced vibrations of structures *Structural Engineers World Congress* Bangalore, India.